HHS Public Access

Author manuscript

Neurobiol Aging. Author manuscript; available in PMC 2024 April 01.

Published in final edited form as:

Neurobiol Aging. 2023 April ; 124: 60–70. doi:10.1016/j.neurobiolaging.2023.01.006.

The Sleep and Wake Electroencephalogram over the Lifespan

Haoqi Sun[1,2,+], **Elissa Ye**[1,^], **Luis Paixao**[1,3], **Wolfgang Ganglberger**[1,+], **Catherine J. Chu**[1], **Can Zhang**[1], **Jonathan Rosand**[1,2], **Emmanuel Mignot**[4], **Sydney S. Cash**[1], **David Gozal**[5], **Robert J. Thomas**[6,*], **M. Brandon Westover**[1,2,*,+]

[1]Department of Neurology, Massachusetts General Hospital, Boston, MA, USA

[2]Henry and Allison McCance Center for Brain Health at Mass General, Boston, MA, USA

[3]Washington University School of Medicine, St. Louis, MO, USA

[4]Center for Sleep Sciences and Medicine, Stanford University, Stanford, CA 94304, USA

[5]Department of Child Health, University of Missouri, Columbia, MO, USA

[6]Department of Medicine, Division of Pulmonary, Critical Care & Sleep, Beth Israel Deaconess Medical Center, Boston, MA, USA

Abstract

Both sleep and wake encephalograms (EEG) change over the lifespan. While prior studies have characterized age-related changes in the EEG, the datasets span a particular age group, or focused on sleep and wake macrostructure rather than the microstructure. Here, we present sex-stratified data from 3,372 community-based or clinic-based otherwise neurologically and psychiatrically healthy participants ranging from 11 days to 80 years of age. We estimate age norms for

Corresponding Author: M. Brandon Westover, M.D. Ph.D., Beth Israel Deaconess Medical Center, Henry and Allison McCance Center for Brain Health, 330 Brookline Avenue, Boston, MA 02215, mwestove@bidmc.harvard.edu, mwestover@mgh.harvard.edu.
[+]Current affiliation: Department of Neurology, Beth Israel Deaconess Medical Center, Boston, MA, USA
[^]Current affiliation: Verily, Cambridge, MA, USA
[*]Co-senior authors.

Disclosure

MBW and SSC are co-founders of Beacon Biosignals. RJT discloses: 1) patent and license/royalties from MyCardio, LLC, for the ECG-spectrogram; 2) patent and license/royalties from DeVilbiss-Drive for an auto-CPAP algorithm; 3) consulting for Jazz Pharmaceuticals, Guidepoint Global and GLG Councils. Other authors declare that they have no conflict of interest.

Credit Author Statement

Haoqi Sun: Formal analysis, Investigation, Roles/Writing - original draft
Elissa Ye: Data curation
Luis Paixao: Writing - review & editing
Wolfgang Ganglberger: Data curation
Catherine J. Chu: Writing - review & editing
Can Zhang: Writing - review & editing
Jonathan Rosand: Writing - review & editing
Emmanuel Mignot: Writing - review & editing
Sydney S. Cash: : Conceptualization, Writing - review & editing
David Gozal: Resources, Writing - review & editing
Robert J. Thomas: Conceptualization, Supervision, Writing - review & editing, Funding acquisition, Resources
M. Brandon Westover: Conceptualization, Supervision, Writing - review & editing, Funding acquisition, Resources

key sleep and wake EEG parameters including absolute and relative powers in delta, theta, alpha, and sigma bands, as well as sleep spindle density, amplitude, duration, and frequency. To illustrate the potential use of the reference measures developed herein, we compare them to sleep EEG recordings from age-matched participants with Alzheimer's disease, severe sleep apnea, depression, osteoarthritis, and osteoporosis. Although the partially clinical nature of the datasets may bias the findings towards less normal and hence may underestimate pathology in practice, age-based EEG reference values enable objective screening of deviations from healthy aging among individuals with a variety of disorders that affect brain health.

Keywords

sleep; aging; electroencephalogram; brain health; age norm

Introduction

Sleep serves a multitude of functions with fundamental importance to both brain and body physiological homeostasis (Krause et al., 2017; Mander et al., 2017a). Sleep structure and circadian rhythms undergo substantial changes with age, reflecting developmental trajectories and aging processes (Mander et al., 2017a). In neonates, the time spent in sleep can exceed 14 hours per day with intermittent sleep and no clear diurnal circadian rhythm (Dias et al., 2018; Eisermann et al., 2013; Jenni et al., 2004). In children and adolescents, the brain undergoes critical changes with maturation. For example, the sleep electroencephalogram (EEG) delta power (1–4Hz) during non-rapid eye movement (NREM) sleep dramatically declines around 11 to 16.5 years of age, attributable to synaptic pruning (Campbell and Feinberg, 2009; Chu et al., 2014). Along with sleep EEG changes, gray matter maturation follows a posterior-to-anterior temporal order (Feinberg et al., 2011), but more precisely from primary sensory and primary motor cortices to posterior association cortices and then to the prefrontal cortex (Chu-Shore et al., 2011; Gogtay et al., 2004). At the other end of the lifespan, older adults typically sleep less during the night, exhibit fragmented sleep architecture, small reductions in rapid eye movement (REM), and major changes in NREM sleep (Luca et al., 2015; Ohayon et al., 2004). Prior to sleep, the eyes-closed awake EEG in the older adults exhibits a slower posterior dominant rhythm (PDR, 8–12Hz); during sleep, the EEG shows decreased slow wave activity (delta, 1–4Hz) in deep sleep (NREM stage 3, N3), reduced spindle density in NREM stage 2 sleep (N2) (Luca et al., 2015; Purcell et al., 2017), and weaker slow-wave-spindle coupling during N2 and N3 stages (Helfrich et al., 2018; Muehlroth et al., 2019). These changes in sleep and awake EEG architecture also reflect underlying structural changes in the brain. For example, early spindle activity is presumed to reflect maturation of thalamocortical structures (Clawson et al., 2016; De Gennaro and Ferrara, 2003). Delta power correlates with cortical thickness in middle frontal, prefrontal, and medial posterior regions (Furrer et al., 2019; Goldstone et al., 2018).

Age-related changes in sleep and awake states in the healthy population can be summarized as an "age norm", i.e., referential ranges of sleep parameters, analogous to growth charts used for tracking weight or height as a function of age in childhood. An age norm represents

a population-level normal trajectory across the lifespan, which can be used to quantify deviations from normal trajectory. Although sleep has been studied across age groups, the literature has mostly focused on age norms of sleep macro-architecture such as total sleep time, bedtime, waking time, and the percentages of sleep stages (Chaput et al., 2018; Dias et al., 2018; Hirshkowitz et al., 2015). However, there is a critical gap for large samples that include a wider age range covering the entire lifespan.

Here, we report the age norm of key sleep and eyes-closed awake EEG parameters based on a cohort of 3,372 participants whose ages range from 11 days to 80 years of age. The age norms provided include EEG spectra, absolute and relative band powers, and spindle density, amplitude, duration, and frequency. To delineate applicability, we also compare sleep characteristics among patients with selected disease states in relation to the age-defined norms. Accordingly, the sleep EEG age norms derived herein provide a quantitative reference to measure deviations from the healthy aging trajectory in individuals with disorders that may affect brain health from the sleep perspective. The cohorts we used here are not “absolutely normal/healthy” (see Datasets below), since they originated from clinical or community populations. For the community-based cohort, since it is hard to track all disease conditions, the age norm could be affected by the common disease prevalence in the community. For the clinical population, although we exclude major diseases that affect sleep and wake EEG, the age norm could be affected by a higher prevalence of sleep disorders if the cohort is derived from clinical patients. Thus, our input populations are “approximately normal” but not “super normal” (i.e., screened to exclude all sleep disorders).

Methods

Datasets

The dataset contains EEGs recorded during overnight polysomnography (PSG) from three datasets: the Collaborative Home Infant Monitoring Effort (CHIME) (Ramanathan et al., 2001), the Chicago Pediatric Community dataset (Pediatric) (Hunter et al., 2016), and the Massachusetts General Hospital Sleep dataset (MGH) (Biswal et al., 2018). In total, these data include 3,396 PSGs from 3,372 participants, ranging in age from 11 days after birth to 80 years. A summary of the combined cohort is provided in Figure 1. Summaries of the individual datasets are provided in Table S1 in the supplementary material. Utilization of the datasets was approved following standard policies including approval by the Institutional Review Board without requiring additional consent.

The CHIME dataset was part of a study aimed at evaluating whether home monitors are effective in identifying episodes of apnea in infants (Ramanathan et al., 2001). Other objectives were to correlate physiological markers, health status, and behavior with the propensity for life-threatening events; and provide important information on the maturation of heart and respiratory function in sleeping infants. Between May 1994 and February 1998, 1,079 infants were enrolled, including healthy term infants, preterm infants weighing less than 1,750 grams at birth, siblings of babies who died from sudden infant death syndrome, and infants who experienced an idiopathic life-threatening event. Here, we used a subset of 405 participants with ages ranging from 11 days to 8 months after birth meeting the

inclusion criteria: (1) age, sleep EEG, and sleep stages were available; and (2) AHI < 30 events per hour based on ranges in healthy infants (Katz et al., 2012), where the AHI was computed based on automatic detection of apnea and hypopnea events (Nassi et al., 2021). Note that in Table S1, the average AHI of CHIME is 1.4/h, which is comparable to previous study (Katz et al., 2012). The flowchart corresponding to the generation of this cohort is shown in Figure S1 in the supplementary material. Sleep EEG was recorded using Healthdyne ALICE 3 software system as part of laboratory polysomnographic recordings, at a sampling frequency of 100Hz. Four EEG channels corresponding to C3-M2, C4-M1, O1-M2, and O2-M1 were included.

The Pediatric dataset was recorded as part of overnight PSG recordings from community recruited children participating in research studies. Among 892 participants, we used a subset of 708 participants meeting the following inclusion criteria (1) age, sex, and AHI are available; and (2) AHI < 15 events per hour. The flowchart for generating this cohort is shown in Figure S2. Ages of the Pediatric dataset are 1 to 13 years. Sleep EEG was recorded using a Nihon-Kohden Polysmith system at a sampling frequency of 100Hz. Four EEG channels, namely C3-M2, C4-M1, O1-M2, and O2-M1 were included.

The MGH cohort is a clinical cohort evaluated in the MGH sleep clinic. We used 2,283 PSGs from 2,259 unique participants based on the following inclusion criteria, designed to ensure that the cohort is representative of normal sleep: (1) age, sex, hypnogram, and apnea-hypopnea index (AHI) were available; (2) diagnostic study (no studies with sleep apnea CPAP titration were included); (3) no significant neurological or psychiatric disease diagnoses within a period five years before to one year after the PSG recording (See Table S2 in the supplementary material); (4) not taking benzodiazepine medications (which affect sleep EEG); and (5) AHI < 15 events per hour. The flowchart generating this cohort is in Figure S3. Ages of patients in the MGH dataset ranged from 13 to 80 years. Sleep EEG was recorded using a Grass recording system at a sampling frequency of 200Hz. Six EEG channels were included in the PSG according to the international 10–20 system: F3-M2, F4-M1, C3-M2, C4-M1, O1-M2, and O2-M1.

Sleep Staging

For the MGH dataset, EEG sleep stages were manually scored by a sleep technician per recording following American Academy of Sleep Medicine (AASM) standards (Berry et al., 2012). Each 30-second epoch is scored as one of the five stages: wake (W), rapid eye movement (REM), NREM stage 1 (N1), NREM stage 2 (N2), and NREM stage 3 (N3). For the Pediatric dataset, sleep stages were similarly scored every 30 seconds for 117 EEGs. There were another 591 EEGs without sleep stages, where automated sleep staging was performed using a previously established algorithm (Sun et al., 2017). For the CHIME dataset, each 30-second epoch was manually scored as one of four stages: wake (W), quiet sleep (Q), active sleep (A), and indeterminate (I) (ANDERS, 1971; Grigg-Damberger, 2016).

EEG Pre-Processing and Artifact Removal

EEG signals in the MGH dataset were downsampled to 100Hz to harmonize the sampling frequency across datasets. EEG signals were notch-filtered at 60Hz to reduce line noise and bandpass filtered from 0.5Hz to 20Hz to reduce muscle artifact. 30-second epochs with absolute amplitude larger than 500μV were removed to minimize movement artifacts. 30-second epochs containing flat signal (voltage < 1 microvolts) for more than 2 seconds were also removed. For the remaining epochs, we trained a linear discriminant analysis (LDA) classifier to classify each epoch into artifact vs. clean. We used total power and the 2nd order difference (for abrupt non-physiological changes) of the spectrum as inputs to the LDA classifier. To train the classifier, we manually labeled each epoch in 20 randomly selected EEGs indicating high total power or non-physiological spectra. Since LDA outputs a probability, we determined the optimal threshold as the one that maximizes the Youden index (sensitivity + specificity − 1) in the receiver operating characteristic (ROC) curve. Visual inspection of the artifact classification confirmed that this achieved an acceptable tradeoff between retaining high quality signal and rejecting artifactual epochs. To reduce the impact of sleep apnea, reduction in oxygen saturation, or respiratory effort-related arousals, we further removed epochs that contained sleep apnea using automated apnea detection from the abdominal respiratory effort belt (Nassi et al., 2021). The total proportions of 30-second epochs removed by these preprocessing procedures were 19% in the MGH dataset, 30% in the Pediatric dataset, and 24% in the CHIME dataset.

Calculation of Age Norms

First, sleep EEG spectrograms were obtained by applying multitaper spectral estimation (Riedel and Sidorenko, 1995) to consecutive 30-second epochs using 4 tapers, and frequency bandwidth 0.46Hz (i.e., time half bandwidth product = 2 × #tapers − 1 = 30s × 0.23Hz). Power spectral density (PSD, $\mu V^2/Hz$) was converted to decibel ($dB = 10 \times \log_{10}(PSD)$). Band powers included delta (1 – 4Hz), theta (4 – 8Hz), alpha (8 – 12Hz), and sigma (11 – 15Hz). We note that the sigma band overlaps with the alpha band, in order to include the lower limit of the frequency range slow spindles. Nevertheless, the sigma band is primarily of interest during N2 sleep, while the alpha band is most relevant to the awake (W) state. To compute relative power in each band, we divide the band power by the total power across the 0.5 – 20Hz range.

We next estimated the spectrum mean and standard deviation using a neural network as a function of age for each sex, sleep stage, and EEG channel, which minimizes the mean squared error (MSE) compared to the actual spectrogram (See Supplementary Method and Figure S8). The motivation for this neural network approach was to take advantage of the large sample size while still ensuring smoothness of estimates between adjacent ages, hence smoothness across all ages. We also note that the number of participants between 6 to 12 months is small (n = 10), where simply using mean and standard deviation leads to biased estimates for this age range. Here, the model is a multi-layer neural network with an exponential linear unit (ELU) activation function (Clevert et al., 2015) to ensure smoothness of the output. The model inputs were the polynomial series of age (age^1, age^2, …, age^K). The model jointly estimates the mean and standard deviation of the power spectral density for each spectral frequency bin. The model was fit using mini-batch stochastic gradient

descent with batch size of 64 30-second epochs and learning rate 0.001. The learning rate was reduced by 10% whenever two consecutive training rounds failed to reduce the loss. Training was stopped when five consecutive training rounds did not reduce the MSE. Hyperparameters tuned for this model included the highest order of polynomial series of age, K, ranging from 5 to 10; the number of hidden layers (2 vs 3); and the number of hidden nodes at each layer, ranging from 50 to 100. We randomly split data into 10% validation and 90% model fitting sets. Hyperparameters that achieved the minimum average loss on the validation set across sleep stages and sexes were $K = 5$; number of hidden layers = 3; and number of hidden nodes = 50 for each hidden layer.

Comparison of Age Norms in Males vs. Females for Pediatric and MGH Datasets

We compared age norms in terms of the means of the age-related spectrograms for males vs. females in Pediatric and MGH datasets. Note that there is no sex information for the CHIME dataset; we included CHIMES data in the analyses for both males and females since it provides context for smoothing, and prior literature reports no significant sex-dependent differences in EEG spectral power in this age range (Myers et al., 2012). Since the neural network model estimates the mean and standard deviation of the age-related spectrogram jointly for males and females, the 95% confidence interval is constructed using mean +/− 1.96 times the standard error (standard deviation / $\sqrt{N(age)}$). The participant number N(age) for each age was determined as the number of participants who with a similar age, was defined as +/−5 age bins around this age, where each age bin was half month for ages younger than 4 years, and one year otherwise.

Sleep Spindle Detection

We used Luna (Purcell et al., 2017) to detect sleep spindles in each channel and to compute spindle density, duration, amplitude, and frequency during N2 sleep (not for N3) for participants > 1 year old, and during Q stage sleep for participants < 1 year old. Using wavelet transformation with wavelet cycle number 12, a spindle was detected if the normalized wavelet coefficient exceeded 4.5 times the mean value across all N2 or Q epochs for that channel and participant. Spindles were required to be between 0.5 seconds to 3 seconds long. Distinguishing between slow and fast spindles is important, due to their different maturational trajectories in the first years of life (D'Atri et al., 2018), and in healthy (Mander et al., 2017b) and pathological (Gorgoni et al., 2016) older adults. Slow spindles are mostly observed in frontal head regions, while fast spindles are mostly at central regions. Therefore, for a given channel and a given age, we used the peak sigma frequency of the spectra at that channel and that age as the center frequency parameter for the Luna spindle detector (see Figure S4 to S7 in the supplementary material for details).

Comparison of the Age Norm to Diseased Patients

To compare with age norms, additional sleep EEGs were extracted from MGH medical records of patients with Alzheimer's disease (AD), severe sleep apnea (SA), depression, osteoarthritis, or osteoporosis. The sleep EEG recordings of each disease group were collected following the same procedure as in those for the age norm. AD was selected because it is associated with disturbed sleep and structural degeneration of the brain (Ju et

al., 2014). SA was selected because it is common in older people (22% in men (Franklin and Lindberg, 2015)) and linked to increased risk of neurodegenerative disease. Depression was selected because of its association with reduced slow wave power (Trivedi and Rush, 2000). Other psychiatric disorders such as schizophrenia were not included due to the small sample size (n=3) in our dataset. Osteoarthritis and osteoporosis were selected as negative controls where we assumed these conditions should not markedly affect sleep EEG. Participants included in disease groups were excluded from the calculation of the age norm. Of note, we did not compare other common systemic disorders including diabetes or hypertension to the age norm since the cohort used to develop the age norm did not exclude them.

The AD cohort included 178 patients with an average age of 72 years of age and 76 were female (43%), based on previously published inclusion criteria (Ye et al., 2020): (1) age at the time of sleep study ≥ 50 years of age; and (2) AD diagnosed based on encounter note or ICD diagnoses either before or 1 year after the sleep study. Exclusion criteria included a diagnosis of tumor/neoplasm, stroke, or developmental delay based on encounter notes or ICD codes within 1 year before or after the sleep study. The SA cohort included 175 patients where the average age is 58 years and 55 patients (31%) were female, satisfying the following inclusion criteria: (1) diagnostic sleep study; (2) AHI > 30 events/hour. The depression cohort included 343 patients where average age is 46 years and 225 were female (66%), with inclusion criterion being diagnosis of depression based on ICD codes either before or 1 year after the sleep study. The osteoarthritis cohort included 115 patients where average age is 64 years and 67 are female (58%), with inclusion criterion being diagnosis of osteoarthritis or degenerative joint diseases based on ICD codes either before or 1 year after the sleep study. The osteoporosis cohort included 135 patients where the average age is 64 years and 101 are female (75%), with inclusion criterion being diagnosis of osteoporosis based on ICD codes either before or 1 year after the sleep study.

For interpretability, we limited the analysis to sleep parameters that are well known in the literature, and whose associations with underlying physiological processes are relatively well studied, including absolute/relative alpha band power in the occipital region during wakefulness; absolute/relative theta band power over the central region during N1 sleep; absolute/relative sigma band power over the central region during N2 sleep; absolute/relative delta band power over the central region during N3 sleep; and spindle characteristics (density, duration, amplitude, frequency) over the central region during N2 sleep.

When comparing each disease entity, for each participant in the diseased group, we matched four participants from the healthy set such that the age difference was less than one year, and participants were of the same sex. The value of four was decided by the largest possible value that still preserves the distributions of ages in the healthy vs. diseased groups, based on a Kolmogorov-Smirnov test $p>0.1$.

Statistical Analyses

For each age, we compared the medians of the EEG parameters for males vs. females that are of similar age (defined above) using the Mann-Whitney U test. The family-wise error rate (FWER) was controlled using the Holm-Bonferroni multiple comparison correction at the 0.05 level. When comparing age norms to parameter values in disease groups, we used

Mann-Whitney U test to test the null hypothesis that the medians of the matched healthy vs. disease groups are the same. The FWER across all diseases and sleep parameters was controlled using the Holm-Bonferroni multiple comparison correction at the 0.05 level.

Results

Age Norm for Spectrum

Age-related EEG spectral changes by sleep and wake state and sex are shown in Figure 2, where the contours in Figure 2c outline regions where sex differences are statistically significant ($p<0.05$, t-test). In the occipital regions, there is a rapid increase in power below 10Hz during the wake state from 0 to 1 year. The peak frequency of the posterior dominant alpha rhythm (PDR) increases to 10Hz until age 20, then slowly decreases to 8 Hz thereafter. For ages < 15 years, there is considerably more delta activity below 4 Hz. Comparison by sex shows that, in the closed-eye awake state, females display higher power at all frequencies except within the alpha band between ages 30 to 50 years.

In general, the sleep spectrograms in all sleep stages show a rapid increase in total power up to 1 year of age, a sharp decrease in total power between ages 2 to 18 years, and a gradual decrease after 18 years of age. During N1, the EEG is generally slower in comparison to wake, and the dominant oscillation is in the theta frequency range. Theta band power increases gradually after 50 years of age. Females show a dip in power across all frequencies between 10 to 18 years of age (adolescent), followed by an increase in power across all frequencies after that.

During N2, the peak frequency of the sigma band at the central channel increases from 11 Hz to 13.5Hz between year 1 and year 20 and remains stable at older ages. Power in the sigma band gradually decreases and becomes indistinct after age 70. Comparison of males vs. females shows females have in general higher power during N2 than males except 10 to 18 years of age.

During N3, delta power is higher compared to N2. Delta power increases sharply from 0 to 1 year, plateaus from 1 to 8 years, and decreases rapidly from 8 to 18 years. Sex-dependent differences are similar to those reported in N2.

During REM, there is more power in the delta range below 4Hz before 18 years of age. At older ages the spectrogram structure is relatively constant. Power in the alpha band can be seen throughout adulthood, reminiscent of the awake state, albeit with reduced power.

Age Norm for Band Powers

Figure 3 shows age vs. absolute power relationships in the delta, theta, alpha, and sigma bands presented in a manner complementary to Figure 2. Total spectral power decreases in childhood and adolescence, mainly because of a decrease in delta power. Sex-dependent changes are shown in the right column. Females have higher central sigma and delta band powers during N2 and N3 stages respectively in most of adulthood from 20 to 75 years of age, with a less steep decrease around 18 to 20 years of age.

In Figure 4, the relative band powers (i.e., band power in percentage divided by total power) show a similar pattern, although sex differences are not as apparent as for measures of absolute power. Relative alpha band power increases until 20 years of age. Relative N2 sigma band power peaks at age 20, remains stable until age 60, and decreases thereafter. Relative delta band power quickly decreases before 2 years of age, then keeps relatively constant (slowly increasing) until 12 years, and slowly decreases thereafter. There is no significant difference in relative band power between males and females, except between 25 to 30 years of age in relative delta band power.

Age Norm for Sleep Spindles

In Figure 5, for spindle parameters in the central channel (solid line) (mostly fast spindle), the spindle frequency shows a sharp decrease from 13.2Hz to below 12Hz in the first year of life, then gradually increase back to 13.5Hz at around 20 years of age and then constant thereafter. The spindle density rises and reaches a maximum at 3 per minute at 18 years for females and 25 years of age for males, then gradually decreases. Spindle duration rapidly rises to longer than 1 second in the first year of life, stabilizes by around 12 years of age, shortens to below 1 second at 18 years, then slowly decreases to around 0.8 second thereafter. Spindle amplitude follows a similar pattern as duration.

For spindle parameters in the frontal channel (dashed line) (mostly slow spindle), since we only have data from the MGH dataset, we cannot describe the changes younger than 13 years of age. The spindle frequency at the frontal channel shows a slow and steady decrease after 13 years of age. The spindle density clearly shows that the peak in frontal channel occurs earlier than that in central channel in both female and male, although the exact peak could not be determined due to lack of data before 13 years of age. Both the spindle duration and amplitude show slow and steady decrease trend.

Females have slightly higher frequency than males from 25 to 50 years. Females have higher spindle density than males from ages 50 to 70 years. Males undergo a decrease in spindle amplitude from 12 to 20 years of age, resulting in higher spindle amplitudes in females than males throughout adulthood. Spindle duration shows no significant differences between female and male.

Age Norm in Early Life

The evolution of EEG spectra from 0 to 36 months after birth is shown in Figure 6. Spectra during the wake state in the occipital region show high delta band power. The PDR in the alpha band begins to emerge around 12 to 16 months. Spectra during quiet sleep in the central region show a single peak frequency in the sigma band beginning around 2 months at ~13Hz (Figure 6c, d, g), which is replaced by lower peak frequency at 11 to 12 Hz starting after 18 months (Figure 6g, green to red curves). Sleep spectra during quiet and active sleep show high delta band power.

Figure 6i–k shows that spindle density, duration and amplitude averaged between C3-M2 and C4-M1 (central channels) are slowly increasing over the first 5 months of life. Figure 6l shows spindle frequency is stable at 13.2Hz over the first 5 months of life.

Comparison of the Age Norm to Diseased Patients

As an exploration of the potential clinical utility of these age-norm measures, we compared average sleep EEG parameters in three disorders against age norms: Alzheimer's disease, sleep apnea, and depression; and two other diseases we considered as negative controls: osteoarthritis and osteoporosis, as shown in Figure 7. Assuming an effect size of 0.3, to reach 80% power, we need at least 109 participants in the diseased group assuming 1:4 ratio for diseased vs. healthy groups, which has been satisfied.

Alzheimer's disease (AD) showed higher theta power during N1, lower relative alpha power during the awake state, lower relative sigma power during N2, lower relative delta power during N3, and lower spindle density during N2. Severe sleep apnea (AHI >30/hour) showed lower spindle density during N2. Depression showed lower relative delta power during N3. As for the two diseases as negative controls, sleep in patients with osteoarthritis is not significantly different from the normative dataset. Sleep in patients with osteoporosis showed higher theta power during N1, but no other significant differences.

It is important to note that patients with one disease could have other known or unknown diseases, and some diseases such as Alzheimer's and sleep apnea are associated. Therefore, the results should not be understood as the effect of solely one disease on the sleep EEG.

Discussion

This study presents empirical age norms for the sleep EEG across the lifespan from 11 days to 80 years. These age norms provide a reference to assess deviations from normal developmental and aging trajectories. The reference values can also be used to analyze which aspects of sleep brain activity deviate from what is normal for age in any given participant. The discussion is organized by different EEG patterns, where early life, childhood, and adulthood are discussed respectively for each pattern, followed by the difference between absolute vs. relative band powers, sex-dependent differences, comparisons to diseased patients, and limitations.

For children under 1 year of age, strong delta oscillations initially occur as "tracé alternant" pattern, consisting of bilateral bursts of high amplitude delta waves superimposed on continuous low amplitude theta activity lasting 3 to 8 seconds. This pattern evolves into continuous diffuse delta (and sometimes theta) activity by early infancy. Sleep spindles are typically present by two months after birth (Jenni et al., 2004), consistent with Figure 6c. Alpha peak frequency is not observable from the spectra in this age range, however it does not rule out transient immature alpha oscillations.

For children above 1 year of age, it is hypothesized that the absolute delta power reflects brain myelin content in developing children from 2 to 12 years of age(LeBourgeois et al., 2019). The reduction in absolute delta power after 12 years of age occurs about the time of puberty, where the human brain undergoes extensive reorganization driven by synaptic plasticity results in a net reduction in synaptic density (Feinberg and Campbell, 2010; Furrer et al., 2019). Alpha peak frequency becomes observable from spectrum beginning from 3 years of age at 8Hz (Figure 6f). Spindles keep increasing in duration and amplitude and

decreasing in frequency across early childhood (McClain et al., 2016), which are related to maturation of thalamocortical structures (Page et al., 2018). Our result about spindle density is consistent with (Scholle et al., 2007). However, our spindle duration result differs from them, possibly due to different methods (wavelet vs. visual) in determining the exact start and end time of a spindle.

In later adulthood, age-related changes in EEG spectral power in NREM sleep have been described (Luca et al., 2015), including decreased absolute delta band power, decreased absolute sigma band power, and increased absolute theta band power. In REM sleep, there is also decreased absolute delta band power. EEG connectivity across brain regions in delta and theta bands during N3 and REM increases with age while EEG connectivity in the sigma band (11–15Hz) during N2 decreases with age (Bouchard et al., 2020; Ujma et al., 2019). An earlier study by Gaudreau et al. examined age-related changes in NREM sleep from 54 participants including children (6 years of age) all the way to middle-age (60 years of age) (Gaudreau et al., 2001). Their documented changes in absolute delta, theta, alpha, and sigma powers are consistent with our findings in Figure 3.

The differences between absolute (Figure 3) vs. relative band powers (Figure 4) reflect the frequency band of interest corrected by theta and delta powers at different ages. This is because at all ages, the power of different brain frequencies follows a 1/f pattern (Ward and Greenwood, 2007), where lower (e.g., delta and theta) frequencies have higher power. The absolute power plots show the raw values without normalization; while the relative plots show the relative proportion of each frequency after accounting for the power in other bands (primarily delta and theta). For this reason, the absolute and relative values follow similar patterns for theta and delta frequencies and dramatically different patterns for higher frequencies at alpha and sigma bands. That being said, an outstanding difference is still present in delta band during N3: the absolute delta power quickly increases (Figure 3) vs. the relative power quickly decreases (Figure 4) under 2 years of age. The increasing absolute delta power is related to the rapid increase in size of neurons and the myelination process (Bosch-Bayard et al., 2022), leading to overall stronger and more synchronized neuronal oscillations. The decreasing relative power is due to the quick decay of tracé alternant pattern at delta band into continuous diffuse delta (and sometimes theta) activity, giving ways to the emergence of oscillations at higher frequencies.

There are several sex-dependent differences. For example, females show a dip in power across all frequencies between 10 to 18 years of age (adolescent) (Figure 2), consistent with an earlier puberty-related power decline in females than that in males (Campbell et al., 2012). Females also show consistently higher absolute sigma band power and delta power during deep sleep after 20 years of age (Figure 3), possibly reflecting both biological (due to hormones) and social differences (higher prevalence of alcohol use and smoking in males). Females have a higher spindle density and amplitude as shown in Figure 5, consistent with the prior literature (Huupponen et al., 2002; Ujma et al., 2014; Warby et al., 2014). The diminished difference between the oldest males and females (> 75 years of age) could be due to survival bias where males have shorter lifespans so that males who survive to older ages are healthier and thus more similar to females. The higher spindle density and amplitude could be related to better correlation between spindle parameters

and intelligence in females (Bódizs et al., 2014; Ujma et al., 2014). However, relative band powers are similar in males and females as indicated by Figure 4, suggesting that sex-dependent changes affect all frequency bands equally. EEG frequencies and power are only a limited subset of many other possible measures of brain health and other measures may not show the same sex-related divergence.

The comparisons to patients with certain diseases provide a practical proof-of-concept example of how the age norms presented herein might be used in practice. Although the age norm cannot be readily used as a diagnostic instrument at the individual level, it could serve as a screening tool when querying a dataset. However, even at individual level, a marked deviation from the norm should reasonably results in further evaluation. Deviation from the age norm is a nonspecific indicator of abnormalities in sleep and brain health, which can be followed up using cognitive tests or neuroimaging biomarker examination. Our results are consistent with prior literature for Alzheimer's disease (Ju et al., 2014), severe obstructive sleep apnea (Mohammadi et al., 2021), and depression (Trivedi and Rush, 2000). For the negative control disease, there could be several hypotheses to explain the elevated theta power during N1 in osteoporosis patients. For example, osteoporosis is a frailty and pain-related disease that is often linked with sleep disturbances (Ensrud et al., 2009), where one line of evidence is the association between chronic insomnia and increased theta power during N1 (Riedner et al., 2016). These hypotheses point to the fact that when comparing diseases to age norms, it is often not only the disease of interest itself that leads to deviations from the age norm, but other comorbidities of the disease of interest must be considered as well.

This study has several important limitations. First, the MGH dataset is a clinical sample, which may bias findings towards "less normal", in which case the age norms may underdiagnose pathology when applied to new individuals. Our effort to exclude patients with neurologic or psychiatric diagnoses and exclude epochs containing sleep apnea mitigates this bias to some extent, but may not address it fully. Second, there is a possible survivor bias in our estimates of age norms at the oldest ages such that those who survive to older ages are more likely to reflect relatively healthier individuals. A survivor bias may also arise from our inclusion criteria including no significant neurological disease near the time of the PSG recording and AHI less than 15 events per hour. There is a higher incidence of neurological disease and higher AHI in the older population, thus reducing the number of samples and biasing them towards better health. Third, we used only one specific sleep spindle detector. While our results are in line with previous findings (in terms of general trends), poor convergent validity of sleep spindle detectors is a known issue (Warby et al., 2014). Therefore, the spindle norms are likely dependent on the specific detector used and its parameters including spectral estimation (wavelet in Luna) and threshold (4.5 times the overall mean normalized wavelet coefficient in Luna). Other limitations include that this was a cross-sectional study where different ages come from different participants with different comorbid conditions. Night-to-night variation in sleep EEG band powers and patterns is also not considered – this dimension would require multi-night data in health across all ages. We also did not study the dynamics of sleep across the night. It is known that there is less N3 and more REM during the latter half of a typical night of sleep. As N3 decreases with age, this trend becomes more attenuated with older age (Purcell et al., 2017). Our study did not

include participants older than 80 years due to limited data beyond this age. Based on an early study of ten centenarians, the average alpha peak frequency was 8.62 Hz, with slower and smaller amplitude total spectral power (Hubbard et al., 1976). Additionally, patients with AD, sleep apnea, or depression are more likely to receive sleep-aid medications or devices, so that the potential trajectory if no treatment intervention is given could be worse than age norms.

Supplementary Material

Refer to Web version on PubMed Central for supplementary material.

Acknowledgements

MBW was supported by the Glenn Foundation for Medical Research and American Federation for Aging Research (Breakthroughs in Gerontology Grant); American Academy of Sleep Medicine (AASM Foundation Strategic Research Award), and by the NIH (R01NS102190, R01NS102574, R01NS107291, RF1AG064312). RT received support from an AASM Foundation Strategic Research Award and RF1AG064312. DG is supported by National Institutes of Health grants HL130984, HL140548, and AG 061824, and a University of Missouri Tier 2 grant. SSC was supported by the NIH (R01NS062092, K24NS088568, and U01NS098968). The Collaborative Home Infant Monitoring Evaluation (CHIME) study was supported by the National Institute of Child Health and Human Development (NICHD) research grant numbers (2 UIO HD28971, HD29067, HD29071, HD29060, HD29056, HD29073, and HD34625).

Data Availability

The raw sleep data from CHIME should be requested from the CHIME committee with a data sharing agreement. The raw sleep data from the Pediatric dataset should be requested from Dr. David Gozal with a data sharing agreement. The raw sleep data from the MGH dataset should be requested from Dr. M. Brandon Westover with a data sharing agreement. All processed age norm data and code to query the age norm are available at https://github.com/mghcdac/sleep_eeg_age_norm with a link to an online age norm query tool. The same age norm is also presented in the supplementary tables S3 to S14.

References

Anders T, 1971. Techniques, and Criteria for Scoring of States of Sleep and Wakefulness in Newborn Infants. A Manual of Standardized Terminology.

Berry RB, Brooks R, Gamaldo CE, Harding SM, Marcus C, Vaughn BV, others, 2012. The AASM manual for the scoring of sleep and associated events. Rules, Terminology and Technical Specifications, Darien, Illinois, American Academy of Sleep Medicine 176, 2012.

Biswal S, Sun H, Goparaju B, Westover MB, Sun J, Bianchi MT, 2018. Expert-level sleep scoring with deep neural networks. J Am Med Inform Assoc 25, 1643–1650. doi: 10.1093/jamia/ocy131. [PubMed: 30445569]

Bódizs R, Gombos F, Ujma PP, Kovács I, 2014. Sleep spindling and fluid intelligence across adolescent development: sex matters. Frontiers in human neuroscience 8, 952. doi: 10.3389/fnhum.2014.00952. [PubMed: 25506322]

Bosch-Bayard J, Biscay RJ, Fernandez T, Otero GA, Ricardo-Garcell J, Aubert-Vazquez E, Evans AC, Harmony T, 2022. EEG effective connectivity during the first year of life mirrors brain synaptogenesis, myelination, and early right hemisphere predominance. NeuroImage 252, 119035. doi: 10.1016/j.neuroimage.2022.119035. [PubMed: 35218932]

Bouchard M, Lina J-M, Gaudreault P-O, Dubé J, Gosselin N, Carrier J, 2020. EEG connectivity across sleep cycles and age. Sleep 43, zsz236. doi: 10.1093/sleep/zsz236.

Campbell IG, Feinberg I, 2009. Longitudinal trajectories of non-rapid eye movement delta and theta EEG as indicators of adolescent brain maturation. Proceedings of the National Academy of Sciences 106, 5177–5180. doi: 10.1073/pnas.0812947106.

Campbell IG, Grimm KJ, De Bie E, Feinberg I, 2012. Sex, puberty, and the timing of sleep EEG measured adolescent brain maturation. Proceedings of the National Academy of Sciences 109, 5740–5743. doi: 10.1073/pnas.1120860109.

Chaput J-P, Dutil C, Sampasa-Kanyinga H, 2018. Sleeping hours: what is the ideal number and how does age impact this? Nature and science of sleep 10, 421. doi: 10.2147/NSS.S163071.

Chu CJ, Leahy J, Pathmanathan J, Kramer M, Cash SS, 2014. The maturation of cortical sleep rhythms and networks over early development. Clinical Neurophysiology 125, 1360–1370. doi: 10.1016/j.clinph.2013.11.028. [PubMed: 24418219]

Chu-Shore CJ, Kramer MA, Bianchi MT, Caviness VS, Cash SS, 2011. Network analysis: applications for the developing brain. Journal of child neurology 26, 488–500. doi: 10.1177/0883073810385345. [PubMed: 21303762]

Clawson BC, Durkin J, Aton SJ, 2016. Form and function of sleep spindles across the lifespan. Neural plasticity. doi: 10.1155/2016/6936381.

Clevert D-A, Unterthiner T, Hochreiter S, 2015. Fast and accurate deep network learning by exponential linear units (elus). arXiv preprint arXiv:1511.07289. doi: 10.48550/arXiv.1511.07289.

D'Atri A, Novelli L, Ferrara M, Bruni O, De Gennaro L, 2018. Different maturational changes of fast and slow sleep spindles in the first four years of life. Sleep medicine 42, 73–82. doi: 10.1016/j.sleep.2017.11.1138. [PubMed: 29458750]

De Gennaro L, Ferrara M, 2003. Sleep spindles: an overview. Sleep medicine reviews 7, 423–440. doi: 10.1053/smrv.2002.0252. [PubMed: 14573378]

Dias CC, Figueiredo B, Rocha M, Field T, 2018. Reference values and changes in infant sleep–wake behaviour during the first 12 months of life: a systematic review. Journal of sleep research 27, e12654. doi: 10.1111/jsr.12654. [PubMed: 29356197]

Eisermann M, Kaminska A, Moutard M-L, Soufflet C, Plouin P, 2013. Normal EEG in childhood: from neonates to adolescents. Neurophysiologie Clinique/Clinical Neurophysiology 43, 35–65. doi: 10.1016/j.neucli.2012.09.091. [PubMed: 23290174]

Ensrud KE, Blackwell TL, Redline S, Ancoli-Israel S, Paudel ML, Cawthon PM, Dam T-TL, Barrett-Connor E, Leung PC, Stone KL, others, 2009. Sleep disturbances and frailty status in older community-dwelling men. Journal of the American Geriatrics Society 57, 2085–2093. doi: 10.1111/j.1532-5415.2009.02490.x. [PubMed: 19793160]

Feinberg I, de Bie E, Davis NM, Campbell IG, 2011. Topographic differences in the adolescent maturation of the slow wave EEG during NREM sleep. Sleep 34, 325–333. doi: 10.1093/sleep/34.3.325. [PubMed: 21358849]

Feinberg I, Campbell IG, 2010. Sleep EEG changes during adolescence: an index of a fundamental brain reorganization. Brain and cognition 72, 56–65. doi: 10.1016/j.bandc.2009.09.008. [PubMed: 19883968]

Franklin KA, Lindberg E, 2015. Obstructive sleep apnea is a common disorder in the population—a review on the epidemiology of sleep apnea. Journal of thoracic disease 7, 1311. doi: 10.3978/j.issn.2072-1439.2015.06.11. [PubMed: 26380759]

Furrer M, Jaramillo V, Volk C, Ringli M, Aellen R, Wehrle FM, Pugin F, Kurth S, Brandeis D, Schmid M, others, 2019. Sleep EEG slow-wave activity in medicated and unmedicated children and adolescents with attention-deficit/hyperactivity disorder. Translational psychiatry 9, 1–8. doi: 10.1038/s41398-019-0659-3. [PubMed: 30664621]

Gaudreau H, Carrier J, Montplaisir J, 2001. Age-related modifications of NREM sleep EEG: from childhood to middle age. Journal of sleep research 10, 165–172. doi: 10.1046/j.1365-2869.2001.00252.x. [PubMed: 11696069]

Gogtay N, Giedd JN, Lusk L, Hayashi KM, Greenstein D, Vaituzis AC, Nugent TF, Herman DH, Clasen LS, Toga AW, others, 2004. Dynamic mapping of human cortical development during childhood through early adulthood. Proceedings of the National Academy of Sciences 101, 8174–8179. doi: 10.1073/pnas.0402680101.

Goldstone A, Willoughby AR, de Zambotti M, Franzen PL, Kwon D, Pohl KM, Pfefferbaum A, Sullivan EV, Müller-Oehring EM, Prouty DE, others, 2018. The mediating role of cortical thickness and gray matter volume on sleep slow-wave activity during adolescence. Brain Structure and Function 223, 669–685. doi: 10.1007/s00429-017-1509-9. [PubMed: 28913599]

Gorgoni M, Lauri G, Truglia I, Cordone S, Sarasso S, Scarpelli S, Mangiaruga A, D'Atri A, Tempesta D, Ferrara M, others, 2016. Parietal fast sleep spindle density decrease in Alzheimer's disease and amnesic mild cognitive impairment. Neural plasticity 2016. doi: 10.1155/2016/8376108.

Grigg-Damberger MM, 2016. The visual scoring of sleep in infants 0 to 2 months of age. Journal of clinical sleep medicine 12, 429–445. doi: 10.5664/jcsm.5600. [PubMed: 26951412]

Helfrich RF, Mander BA, Jagust WJ, Knight RT, Walker MP, 2018. Old brains come uncoupled in sleep: slow wave-spindle synchrony, brain atrophy, and forgetting. Neuron 97, 221–230. doi: 10.1016/j.neuron.2017.11.020. [PubMed: 29249289]

Hirshkowitz M, Whiton K, Albert SM, Alessi C, Bruni O, DonCarlos L, Hazen N, Herman J, Katz ES, Kheirandish-Gozal L, others, 2015. National Sleep Foundation's sleep time duration recommendations: methodology and results summary. Sleep health 1, 40–43. doi: 10.1016/j.sleh.2014.12.010. [PubMed: 29073412]

Hubbard O, Sunde D, Goldensohn ES, 1976. The EEG in centenarians. Electroencephalography and Clinical Neurophysiology 40, 407–417. doi: 10.1016/0013-4694(76)90192-9. [PubMed: 56267]

Hunter SJ, Gozal D, Smith DL, Philby MF, Kaylegian J, Kheirandish-Gozal L, 2016. Effect of sleep-disordered breathing severity on cognitive performance measures in a large community cohort of young school-aged children. American journal of respiratory and critical care medicine 194, 739–747. doi: 10.1164/rccm.201510-2099OC. [PubMed: 26930303]

Huupponen E, Himanen S-L, Värri A, Hasan J, Lehtokangas M, Saarinen J, 2002. A study on gender and age differences in sleep spindles. Neuropsychobiology 45, 99–105. doi: 10.1159/000048684. [PubMed: 11893867]

Jenni OG, Borbély AA, Achermann P, 2004. Development of the nocturnal sleep electroencephalogram in human infants. American Journal of Physiology-Regulatory, Integrative and Comparative Physiology 286, R528–R538. doi: 10.1152/ajpregu.00503.2003. [PubMed: 14630625]

Ju Y-ES, Lucey BP, Holtzman DM, 2014. Sleep and Alzheimer disease pathology—a bidirectional relationship. Nature Reviews Neurology 10, 115–119. doi: 10.1038/nrneurol.2013.269. [PubMed: 24366271]

Katz ES, Mitchell RB, D'Ambrosio CM, 2012. Obstructive sleep apnea in infants. American journal of respiratory and critical care medicine 185, 805–816. doi: 10.1164/rccm.201108-1455CI. [PubMed: 22135346]

Krause AJ, Simon EB, Mander BA, Greer SM, Saletin JM, Goldstein-Piekarski AN, Walker MP, 2017. The sleep-deprived human brain. Nature Reviews Neuroscience 18, 404–418. doi: 10.1038/nrn.2017.55. [PubMed: 28515433]

LeBourgeois MK, Dean DC, Deoni SC, Kohler M, Kurth S, 2019. A simple sleep EEG marker in childhood predicts brain myelin 3.5 years later. NeuroImage 199, 342–350. doi: 10.1016/j.neuroimage.2019.05.072. [PubMed: 31170459]

Luca G, Haba Rubio J, Andries D, Tobback N, Vollenweider P, Waeber G, Marques Vidal P, Preisig M, Heinzer R, Tafti M, 2015. Age and gender variations of sleep in subjects without sleep disorders. Annals of medicine 47, 482–491. doi: 10.3109/07853890.2015.1074271. [PubMed: 26224201]

Mander BA, Winer JR, Walker MP, 2017a. Sleep and human aging. Neuron 94, 19–36. doi: 10.1016/j.neuron.2017.02.004. [PubMed: 28384471]

Mander BA, Zhu AH, Lindquist JR, Villeneuve S, Rao V, Lu B, Saletin JM, Ancoli-Israel S, Jagust WJ, Walker MP, 2017b. White matter structure in older adults moderates the benefit of sleep spindles on motor memory consolidation. Journal of Neuroscience 37, 11675–11687. doi: 10.1523/JNEUROSCI.3033-16.2017. [PubMed: 29084867]

McClain IJ, Lustenberger C, Achermann P, Lassonde JM, Kurth S, LeBourgeois MK, 2016. Developmental changes in sleep spindle characteristics and sigma power across early childhood. Neural plasticity 2016. doi: 10.1155/2016/3670951.

Mohammadi H, Aarabi A, Rezaei M, Khazaie H, Brand S, 2021. Sleep spindle characteristics in obstructive sleep apnea syndrome (OSAS). Frontiers in neurology 134. doi: 10.3389/fneur.2021.598632.

Muehlroth BE, Sander MC, Fandakova Y, Grandy TH, Rasch B, Shing YL, Werkle-Bergner M, 2019. Precise slow oscillation–spindle coupling promotes memory consolidation in younger and older adults. Scientific reports 9, 1–15. doi: 10.1038/s41598-018-36557-z. [PubMed: 30626917]

Myers M, Grieve P, Izraelit A, Fifer W, Isler J, Darnall R, Stark R, 2012. Developmental profiles of infant EEG: overlap with transient cortical circuits. Clinical neurophysiology 123, 1502–1511. doi: 10.1016/j.clinph.2011.11.264. [PubMed: 22341979]

Nassi T-E, Ganglberger W, Sun H, Bucklin AA, Biswal S, Van Putten M, Thomas R, Westover B, 2021. Automated Scoring of Respiratory Events in Sleep with a Single Effort Belt and Deep Neural Networks. IEEE Transactions on Biomedical Engineering 69, 2094–2104. doi: 10.1109/TBME.2021.3136753.

Ohayon MM, Carskadon MA, Guilleminault C, Vitiello MV, 2004. Meta-analysis of quantitative sleep parameters from childhood to old age in healthy individuals: developing normative sleep values across the human lifespan. Sleep 27, 1255–1273. doi: 10.1093/sleep/27.7.1255. [PubMed: 15586779]

Page J, Lustenberger C, Fröhlich F, 2018. Social, motor, and cognitive development through the lens of sleep network dynamics in infants and toddlers between 12 and 30 months of age. Sleep 41, zsy024. doi: 10.1093/sleep/zsy024.

Purcell S, Manoach D, Demanuele C, Cade B, Mariani S, Cox R, Panagiotaropoulou G, Saxena R, Pan J, Smoller J, others, 2017. Characterizing sleep spindles in 11,630 individuals from the National Sleep Research Resource. Nature communications 8, 1–16. doi: 10.1038/ncomms15930.

Ramanathan R, Corwin MJ, Hunt CE, Lister G, Tinsley LR, Baird T, Silvestri JM, Crowell DH, Hufford D, Martin RJ, others, 2001. Cardiorespiratory events recorded on home monitors: comparison of healthy infants with those at increased risk for SIDS. Jama 285, 2199–2207. doi: 10.1001/jama.285.17.2199. [PubMed: 11325321]

Riedel KS, Sidorenko A, 1995. Minimum bias multiple taper spectral estimation. IEEE Transactions on Signal Processing 43, 188–195. doi: 10.1109/78.365298.

Riedner BA, Goldstein MR, Plante DT, Rumble ME, Ferrarelli F, Tononi G, Benca RM, 2016. Regional patterns of elevated alpha and high-frequency electroencephalographic activity during nonrapid eye movement sleep in chronic insomnia: a pilot study. Sleep 39, 801–812. doi: 10.5665/sleep.5632. [PubMed: 26943465]

Scholle S, Zwacka G, Scholle H, 2007. Sleep spindle evolution from infancy to adolescence. Clinical neurophysiology 118, 1525–1531. doi: 10.1016/j.clinph.2007.03.007. [PubMed: 17475551]

Sun H, Jia J, Goparaju B, Huang G-B, Sourina O, Bianchi MT, Westover MB, 2017. Large-Scale Automated Sleep Staging. Sleep 40, zsx139. doi: 10.1093/sleep/zsx139.

Trivedi M, Rush AJ, 2000. Temporal characteristics of delta activity during NREM sleep in depressed outpatients and healthy adults: group and sex effects. Sleep 23, 1. doi: 10.1093/sleep/23.5.1c.

Ujma PP, Konrad BN, Genzel L, Bleifuss A, Simor P, Pótári A, Körmendi J, Gombos F, Steiger A, Bódizs R, others, 2014. Sleep spindles and intelligence: evidence for a sexual dimorphism. Journal of Neuroscience 34, 16358–16368. doi: 10.1523/JNEUROSCI.1857-14.2014. [PubMed: 25471574]

Ujma PP, Konrad BN, Simor P, Gombos F, Körmendi J, Steiger A, Dresler M, Bódizs R, 2019. Sleep EEG functional connectivity varies with age and sex, but not general intelligence. Neurobiology of Aging 78, 87–97. doi: 10.1016/j.neurobiolaging.2019.02.007. [PubMed: 30884412]

Warby SC, Wendt SL, Welinder P, Munk EG, Carrillo O, Sorensen HB, Jennum P, Peppard PE, Perona P, Mignot E, 2014. Sleep-spindle detection: crowdsourcing and evaluating performance of experts, non-experts and automated methods. Nature methods 11, 385–392. doi: 10.1038/nmeth.2855. [PubMed: 24562424]

Ward LM, Greenwood PE, 2007. 1/f noise. Scholarpedia 2, 1537. doi: 10.4249/scholarpedia.1537.

Ye E, Sun H, Leone MJ, Paixao L, Thomas RJ, Lam AD, Westover MB, 2020. Association of sleep electroencephalography-based brain age index with dementia. JAMA network open 3, e2017357–e2017357. doi: 10.1001/jamanetworkopen.2020.17357. [PubMed: 32986106]

Highlights

- There is a gap in the sleep literature: studies focusing on sleep EEG changes across the entire lifespan.
- Sex-stratified data from 3,372 participants ranging from 11 days to 80 years old.
- The results provide reference sleep EEG parameters, quantifying deviations from normal.

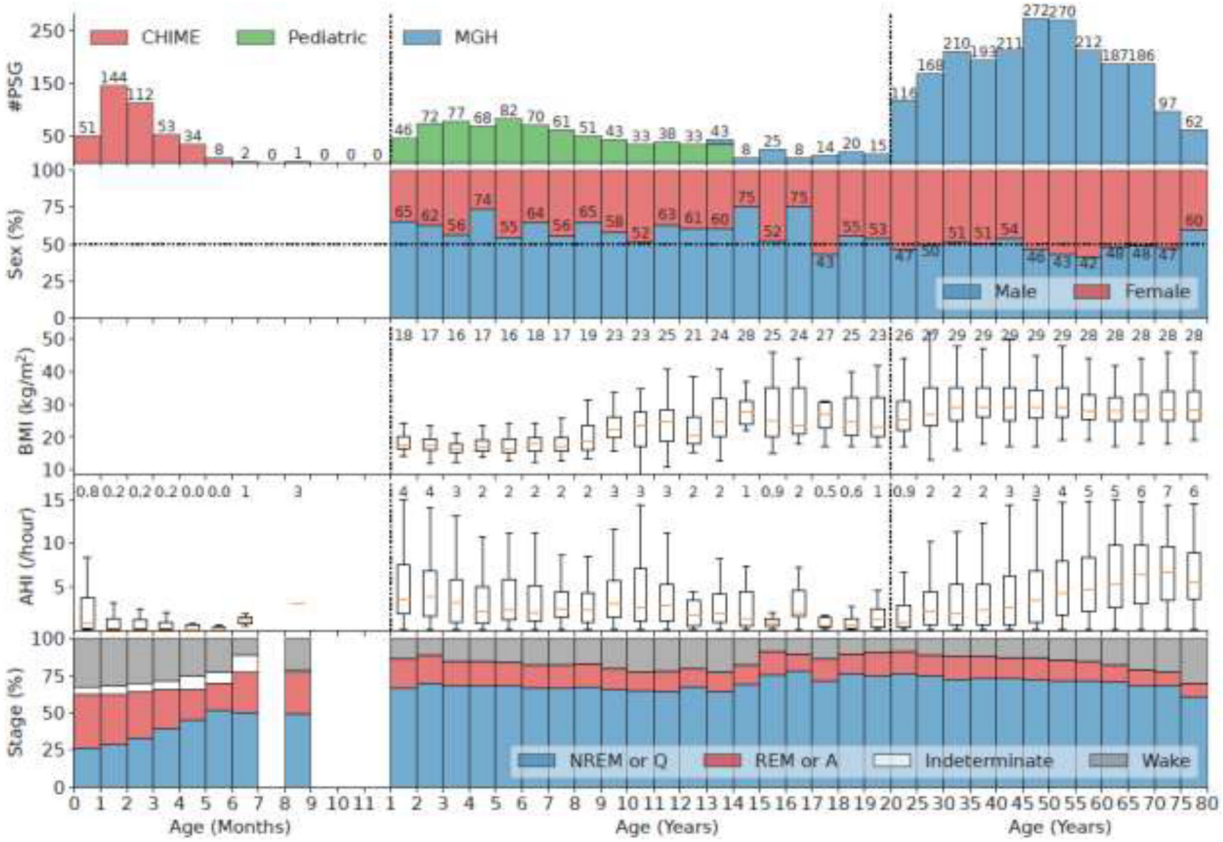

Figure 1.

Characteristics of the combined cohort. The x-axis is age divided into 3 parts: 0 to 11 months (increment 1 month), 1 to 19 years (increment 1 year), and 20 to 80 years (increment 5 years). The two vertical dashed lines in the panels indicate the division. The first panel is the histogram of PSGs in different age bins. Different colors indicate different datasets which are stacked when overlapping age bins exist. The second panel shows the percentage of male and female in each age bin. The third panel shows the boxplots of BMI in each age bin when available. The middle orange line of each box indicates the median, the boundary of the box indicates the 75% and 25% percentiles, and the whiskers extend the box by 1.5 times the inter-quartile range. The numbers at the top show the median values. The fourth panel shows the boxplots of AHI in each age bin. The bottom panel shows the distribution of sleep stages. For the CHIME dataset, the sleep stages are quiet sleep (Q) which resembles NREM, active sleep (A) which resembles REM, indeterminate or transitional (I), and awake (W).

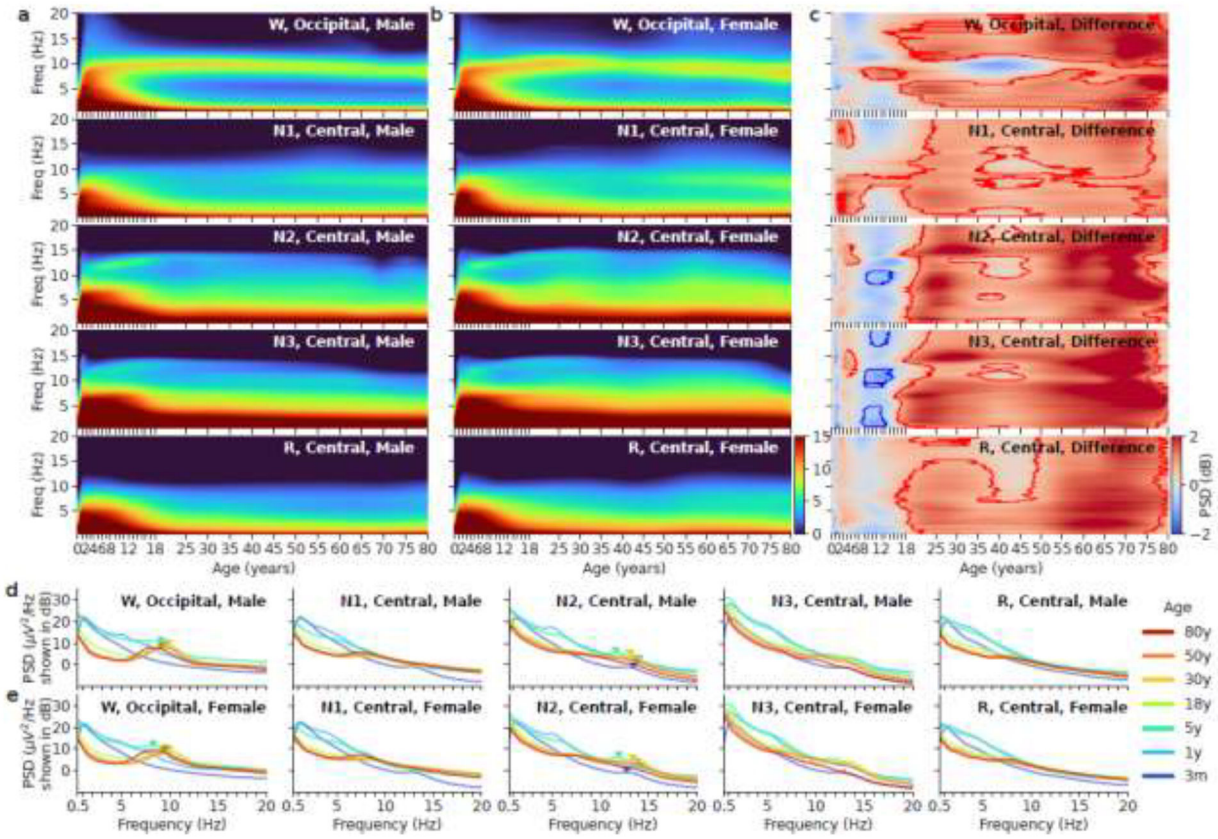

Figure 2.

Left two columns: Age vs. spectrum for all five sleep stages in males (a) vs. females (b). The x-axis is age after birth in years. The y-axis is frequency from 0.5Hz to 20Hz. The power is shown in the unit of decibels. (c) Difference between males and females in the Pediatric dataset and MGH dataset. Red means females have higher mean power; blue means males have higher mean power. The contours outline regions within which sex differences are statistically significant. (d) Example spectra at 3 months, 1, 5, 18, 30, 50, and 80 years of age in males and the five sleep stages. The triangle markers indicate alpha peak frequency in W and sigma peak frequency in N2. (e) Example spectra at 3 months, 1, 5, 18, 30, 50, and 80 years of age in females and the five sleep stages.

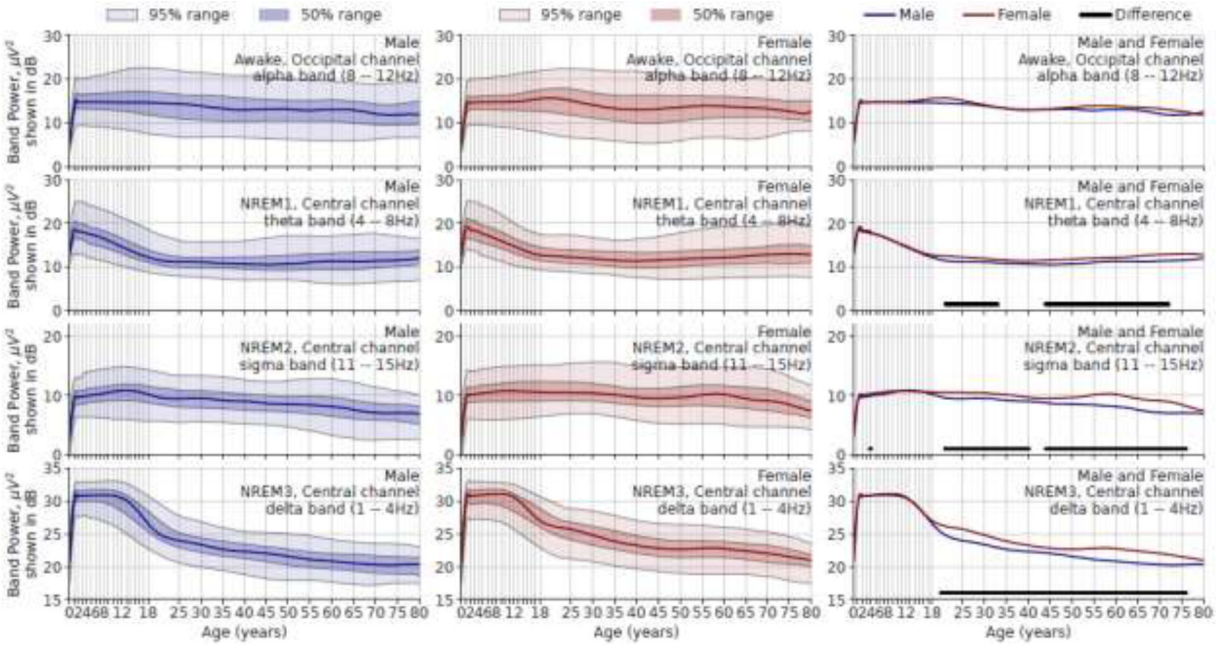

Figure 3.

Age vs. absolute band power in μV^2 (but shown in decibels). Rows show different frequency bands in different sleep stages. Left column, males; middle column, females; right column, both sexes. The ranges are derived from population data. In the right column, the solid lines beneath the red and blue curves indicate age ranges where median values for males and females are significantly different after Holm-Bonferroni correction.

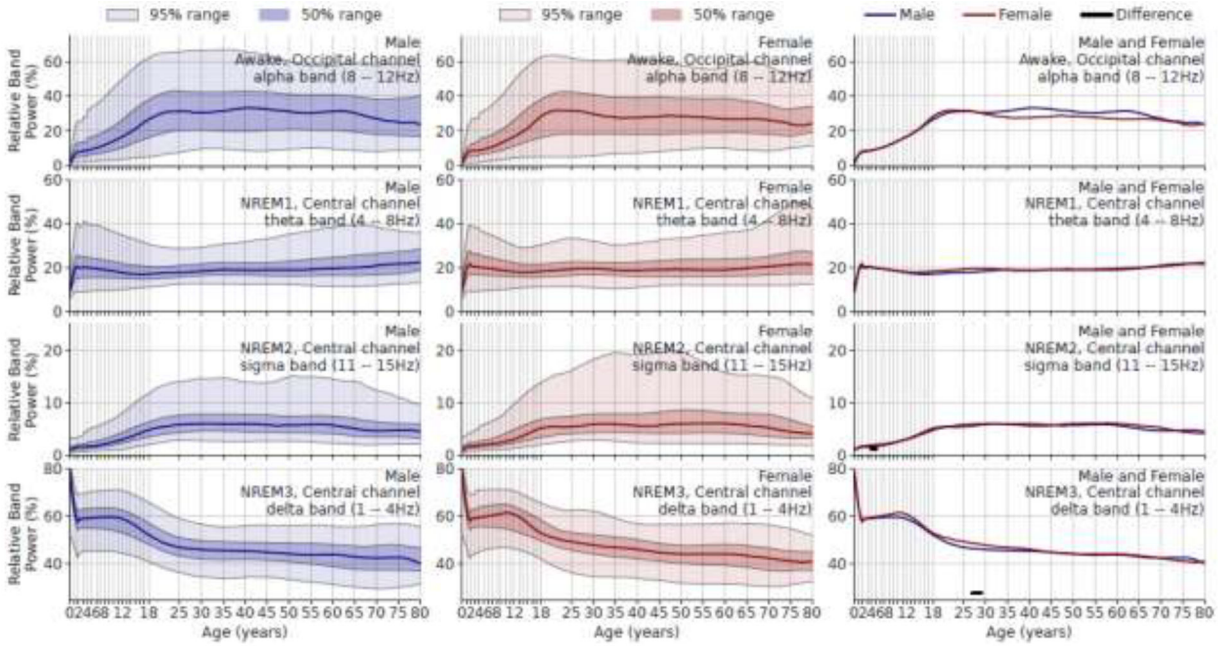

Figure 4.

Age vs. relative band power (%). Rows show frequency bands in different sleep stages. Left column: males; middle column: females; right column: comparing sexes. Solid underlines indicate the age range where the median parameters of male and female are significantly different after Holm-Bonferroni correction.

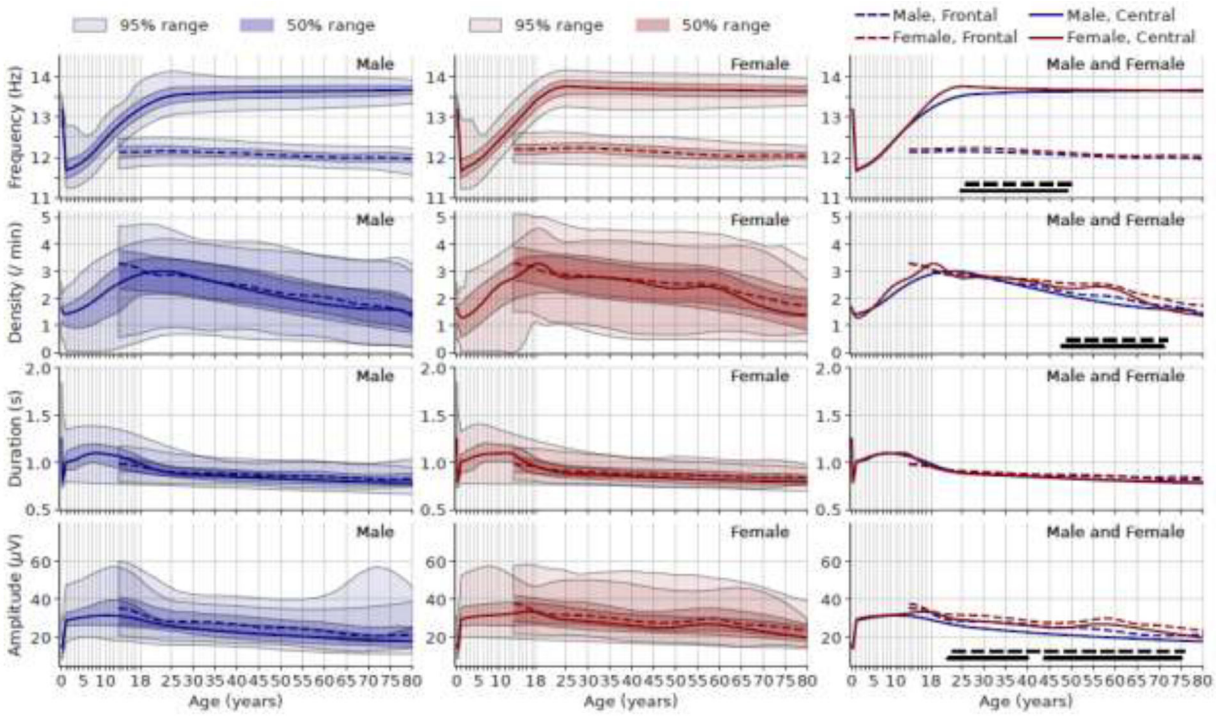

Figure 5.

Age vs. spindle frequency (1st row), density (2nd row), duration (3rd row), and amplitude (4th row). Left column: males; middle column females; right column: both sexes combined. The solid lines represent spindle parameters from the average of C3-M2 and C4-M1 (central channels). The dashed lines represent spindle parameters from the average of F3-M2 and F4-M1 (frontal channels). In the right column, the lines at the bottom (dashed for frontal channel, solid for central channel) indicate age range where the median value of males and females are significantly different after Holm-Bonferroni correction.

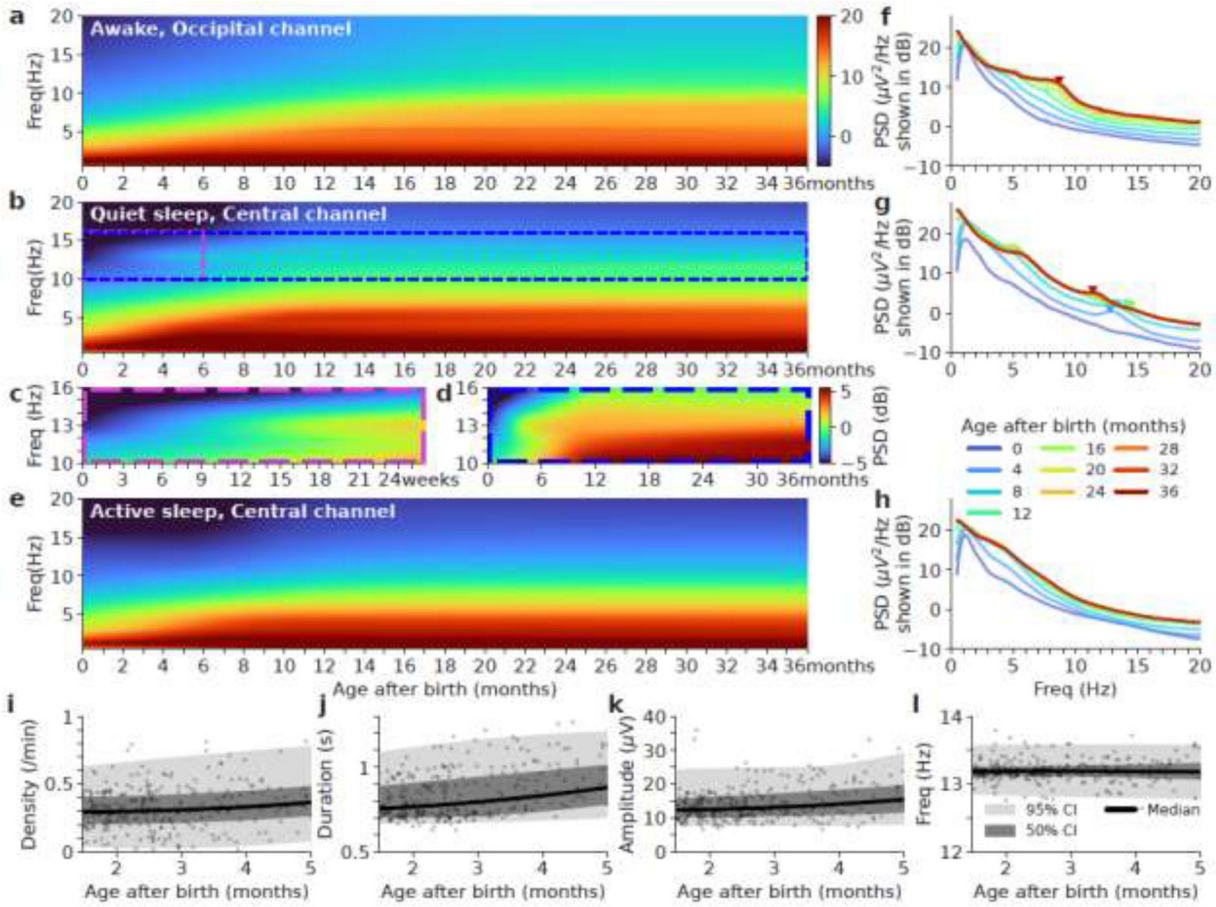

Figure 6.

Age-related spectra for wake (a), quiet sleep (Q or NREM) (b), and active sleep (A or REM) (e) in the first 3 years of life. Panel c and d we show zooms of areas of white and blue regions respectively with a different color range to highlight the subtle spectral changes. (f, g, h) The averaged spectra for each 3-month bin for each sleep stage respectively. The x-axis is frequency in Hz. The y-axis is power spectral density (PSD) in decibels (dB). The triangle markers indicate alpha peak frequency in wake and sigma peak frequency in quiet sleep. (i, j, k, l) Age vs. spindle density, duration, amplitude, and frequency during quiet sleep in the central channel for the first 5 months of life. Spindles parameters are obtained from the average of C3-M2 and C4-M1 (central channels). Pearson's correlation p-values are significant for density, duration, amplitude, except for frequency.

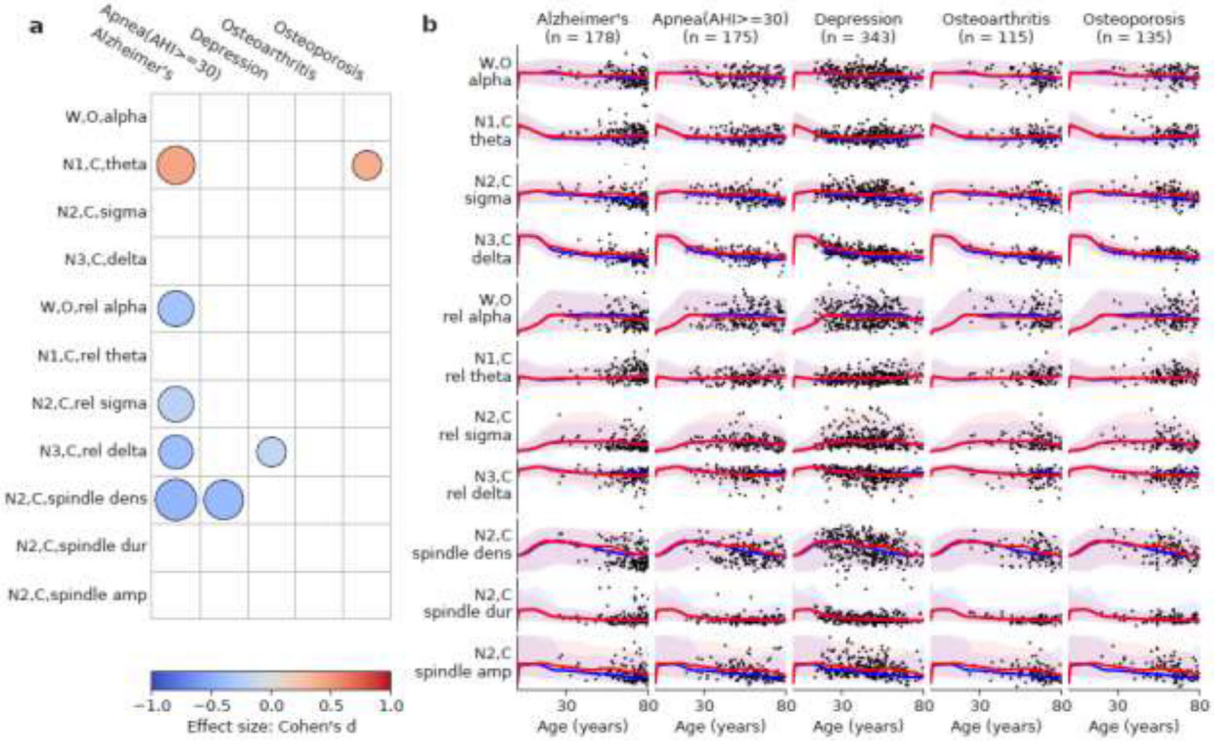

Figure 7.

(a) Comparison against age norms of several sleep parameters (y-axis) in five diseases (x-axis). The color of the circles indicates effect size (Cohen's d). Red color means the disease group has an elevated value relative to the age norm, and vice versa for blue. The radius of the circles indicates the p-value of the difference ($1 - \sqrt[6]{p}$). Only significant differences after Holm-Bonferroni correction are shown. (b) The scatter plot of age vs. sleep EEG patterns for patients with these five diseases. The curves represent age norms (red is female and blue is male). The shaded areas represent the 95% range of the sleep EEG patterns.